

Bayesian inference of prehistoric population dynamics from multiple proxies: a case study from the North of the Swiss Alps

Martin Hinz^{1,2,*} Joe Roe¹ Julian Laabs³ Caroline Heitz³ Jan Kolář^{4,5}

28 Mai, 2022

Abstract

Robust estimates of population are essential to the study of human–environment relations and socio-ecological dynamics in the past. Population size and density can directly inform reconstructions of prehistoric group size, social organisation, economic constraints, exchange, and political and social institutions. In this pilot study, we present an approach that we believe can be usefully transferred to other regions, as well as refined and extended to greatly advance our understanding of prehistoric demography. Here, we present a Bayesian hierarchical model that uses Poisson regression and state-space representation to produce absolute estimates of past population size and density. Using the area North of the main ridge of the Swiss Alps in prehistoric times (7000–1000 BCE) as a case study, we show that combining multiple proxies (site counts, radiocarbon dates, dendrochronological dates, and landscape openness) produces a more robust reconstruction of population dynamics than any single proxy alone. The model's estimates of the credibility of its prediction, and the relative weight it affords to individual proxies through time, give further insights into the relative reliability of the evidence currently available for paleodemographic research. Our prediction of population development of the case study area accords well with the current understanding in the wider literature, but provides a more precise and higher-resolution estimate that is less sensitive to spurious fluctuations in the proxy data than existing approaches, especially the popular summed probability distribution of radiocarbon dates. The archaeological record provides several potential proxies of human population dynamics, but individually they are inaccurate, biased, and sparse in their spatial and temporal coverage. Similarly, current methods for estimating past population dynamics are often simplistic: they work on limited spatial scales, tend to rely on a single proxy, and are rarely able to infer population size or density in absolute terms. In contemporary demography, it is becoming increasingly common to use Bayesian statistics to estimate population trends and project them into the future. The Bayesian approach is popular because it offers the possibility of combining heterogeneous data, and at the same time quantifying the uncertainty and credibility attached to forecasts. These same characteristics make it well-suited to applications to archaeological data in paleodemographic studies.

¹ Institute of Archaeological Sciences, University of Bern

² Oeschger Centre for Climate Change Research, University of Bern

³ CRC 1266 - Scales of Transformation, University of Kiel

⁴ Department of Vegetation Ecology, Institute of Botany of the Czech Academy of Sciences

⁵ Institute of Archaeology and Museology, Faculty of Arts, Masaryk University

* Correspondence: Martin Hinz <martin.hinz@iaw.unibe.ch>

Keywords: Prehistoric demography; Bayesian modelling; Multi-proxy; Settlement dynamics

Highlights: - Bayesian modelling can integrate multiple, heterogeneous population proxies from the archaeological record - Our initial model produces more robust, high-resolution estimates of past population dynamics than previous, single-proxy approaches - We provide absolute estimates of population size and density on the area north of the Swiss Alps in prehistoric times (7000–1000 BCE)

1 Introduction

1.1 Prehistoric demography

Prehistorians have long recognised demography as a fundamental force in human cultural evolution (Childe, 1936). However, despite decades of interest in the demographic dynamics of prehistoric societies, concrete estimates of population size and population density before written records remain elusive. Though the archaeological record provides multiple possible demographic proxies (Hassan, 1981), lack of access to this data, and a lack of methodological tools for turning it into quantitative estimates, has often left the conclusions drawn from it vague and superficial (Hassan, 1981). As a result, ‘expert estimates’ transferred from ethnographic parallels have often taken the place of direct inference from archaeological evidence Turchin et al. (2015).

Early attempts to estimate the size and density of prehistoric populations from archaeological remains were made by Hack (1942), Colton (1949), Frankfort (1950) and Cook (1946). Cook and Heizer Cook and Heizer (1968) and Naroll (1962) provided rules derived from ethnographic contexts for estimating the size of prehistoric populations. Cook and Heizer (1966) also made the first attempt to estimate the population growth rate during the Neolithic (Hassan, 1981). These approaches became increasingly common after the 1960s, with the emergence of processual archaeology and its focus on human–environment relations and population ecology (Hassan, 1981).

Following a spell out of fashion with the post-processual turn, prehistoric demography has experienced a revival in recent years as part of the cultural evolution paradigm (Riede, 2009 and others in same issue; Shennan, 2000). Part of this resurgence can be explained by a renewed interest in human–environment relations and human impact on the natural environment, which necessarily requires an assessment of population size. Kintigh et al. (2014), for example, list human influence, dominance, population size, and population growth amongst their ‘grand challenges’ for archaeology in the 21st century.

But methodological advances have certainly also played a role. In the last decade, the ‘dates as data’ technique (Rick, 1987), which uses the frequency of radiocarbon dates as a proxy for population dynamics, was taken up and significantly developed in a series of publications from the UCL group (e.g. Shennan et al., 2013), and has since been widely applied to archaeological contexts around the world (Crema, 2022).

The ‘dates as data’ or summed radiocarbon approach has contributed greatly to our understanding of prehistoric demography, but it is not without its critics Carleton and Groucutt (2021). While the methodology continues to evolve and address these critiques (Crema, 2022), it remains subject to certain fundamental problems common to all approaches that rely on a single proxy Schmidt et al. (2021). We believe that these problems cannot be overcome by methodological refinements in this area alone. Instead, the Bayesian approach we develop in this paper offers a robust, quantitative methodology for inferring prehistoric population dynamics from multiple proxies, including summed radiocarbon dates.

2 Background

2.1 Existing approaches to population estimation

Müller and Diachenko (2019) have compiled a list proxies currently used for the estimation of population size in prehistory. These can be roughly divided into three groups: ethnographic analogies; deductive estimates from ecological/economic factors; and the interpolation of frequencies of archaeological features (e.g. settlements, structures, individual finds). Three basic problems are common to all these approaches:

1. **Reliance on single proxy:** Most investigations are using only one source of evidence. Although multi-proxy approaches exist, in such cases the individual proxies only serve to support each other or the proxy used as the main estimator. There is no explicit combination of results to reduce the inaccuracy and biases inherent to single proxies.
2. **Uncertainty in measurements:** All archaeological evidence comes with an inherent uncertainty which is carried through to derived measurements. However, in most studies of prehistoric population,

individual curves are presented as estimates, and the potential error associated with these estimates is almost never specified.

3. **Lack of a transfer function:** By ‘transfer function’, we mean something that allows for the proxy data to be interpreted in terms of actual population size or density. This could be absolute, i.e. a numerical estimate of population, or relative, i.e. a means of scaling changes in the proxy value to changes in population. Lack of a suitable frameworks and ‘calibration’ data means that this is rarely presented alongside proxy estimates. In the best case scenario, there will be a qualitative assessment of the informative value of the proxy, but this does not sufficiently account for the complex nature of archaeological data.

Furthermore, the types of archaeological data commonly used as population proxies share a number of problematic characteristics. They are:

- **Limited:** We have only incomplete data that can be used for these purposes, and they are usually not very informative.
- **Unevenly distributed:** For example, although there is a good data on settlement frequencies for some regions, and these are sometimes have a very high temporal resolution, these regions are very unevenly distributed over time and space.
- **Noisy:** Frequently individual proxies are strongly influenced by factors unrelated to population, for example taphonomic conditions or depositional biases.
- **Unreliable:** Research strategies, research history and varying levels of resources available to researchers strongly affect the nature of compiled datasets. As a result, systematic distortions are the rule rather than the exception.
- **Heterogeneous:** A wide range of proxies can potentially inform us about population dynamics, all with different spatio-temporal scales, granularity, information value, scales, and data formats.
- **Indirect:** We will never have direct data on prehistoric population; only proxy data that is thought to be a reasonable substitute for it. The transfer functions that link the proxy data with the desired quantity (population) are unknown. At best, they may be estimated by comparison with historical examples or the (ethnographic) present. However, since living conditions, circumstances and economic parameters differ greatly between the recent history and prehistory, these transfer functions can only be considered a rough first approximation.
- **Contradictory:** When considering several proxies, differences in transfer functions, data quality and noisiness inevitably lead to different results. The most common way to deal with this is to reject certain proxies for a certain time periods, but this is not performed on a consistent or quantitative basis.

Here we argue that many, if not all, of these problems can be ameliorated through a) the explicit, quantitative integration of multiple proxies; and b) the use of a Bayesian approach to take account of and estimate uncertainty.

2.2 Hierarchical Bayesian demographic models

Many of the problems with archaeological population proxies are also encountered in contemporary demography. In response, demographers have increasing turned to Bayesian methods to estimate and forecast contemporary population dynamics. For example, Bryant and Zhang (2018) consider Bayesian data modelling a solution to exactly the kind of problems that affect archaeological data. Specifically, Bayesian approaches are well suited for limited, unreliable and noisy data. Various sources of data, even contradictory data, can be brought into a common framework and used to support one another. These methods also provide a quantitative estimate of the likelihood and uncertainty of the model’s resulting predictions (or in our case retro-dictions). Bayesian approaches are also capable of accounting for spatially and temporally incomplete data: where this data is missing, the uncertainty automatically increases, but this does not prevent general modelling and estimation. Finally, hierarchically-structured model suites, in which sub-models are created for each individual proxy, can be used to estimate transfer functions between individual proxies and the value to be modelled, thanks to the interaction of a large number of data sources and evidence.

This modeling technique can thus be used to combine different lines of evidence horizontally and vertically and in this way combine their results into a common conclusion and estimate, which at the same time includes

an estimation of their reliability: if the data contradict each other, the overall reliability will be lower. If they support each other, the confidence interval will be smaller. And if there is no systematic bias that affects all data sources to the same extent, it should be possible to arrive at the most reliable estimate possible through the most heterogeneous set of data sources.

The well-established application of a Bayesian approach in radiocarbon calibration, where it is used to model radiometric uncertainty based on stratigraphic information, represents a very similar use case in archaeology. More recently, archaeologists have also used Bayesian modelling techniques as a tool for testing hypotheses relating to demographic trends or underlying models based on ^{14}C data (e.g. Crema and Shoda, 2021). This approach differs from the one presented in this paper in that, in these analyses, deductive models are generated and their plausibility is tested on the basis of ^{14}C data only. This is a clear step forward in the direction of a model-based, and thus scientific, analysis. However, the use of only one proxy, and its use exclusively for testing hypotheses developed independently, creates problems comparable to those of the inductive approaches used so far: due to the lack of a combination with other indicators, one is limited to the problems and conditions of sum calibration as a tool. Furthermore, this approach loses significant potential information that would be gained by a direct evaluation of the time series. Thus, the credibility of a model can only be checked as a whole, without the dynamic developments that can arise in the course of demographic processes being represented. We would like to better exploit the capabilities of Bayesian hierarchical models through a combination of inductive data analysis and model-passed data integration of different proxies.

Here, we attempt to make Bayesian hierarchical techniques usable for archaeological reconstructions. In addition to a presentation of the basics and possible procedures, we want to show in the following, in a reproducible and practical form using a case study, how Bayesian methods can also make a decisive contribution to a better assessment of population development. These assessments are crucial for the reconstruction of the human past, even in for periods for which we only have very patchy, noisy and unreliable data.

2.3 Assumptions of a Bayesian approach

The basis of Bayesian statistics is the premise that there is always some prior assumption about the probability of an event, even if it may be very rough. This assumption is then adjusted by observing the data. The concept of probability is not derived from theoretical, infinitely repeatable random experiments or distributions, but from the direct confrontation of the pre-assumptions (priors) with the available data. This involves checking how credible these prior assumptions are with regard to the available data (likelihood, see also Bryant and Zhang, 2018, p. 66). A small amount of data leads to a broad probability distribution that is not strongly localised and restricted. The intuitive procedure is thereby the shifting of credibility through evidence.

At the heart of all Bayesian statistics is therefore the concept of updating a given prior assumption with new data and expressing this in probabilities (cf. also Kruschke, 2015, especially 15–25). Our assumptions about the demographic development of the past must naturally be very conservative. In the logic of the basic Bayesian equation, these assumptions represent the prior (probability). In conjunction with the data that are included as the likelihood of the prior, a posterior (probability) results, which represents the Bayesian model learning from data. It is also in the nature of the approach that in real applications there is no point prediction, but in most cases a probability distribution for the prediction. Thus, we simultaneously obtained a result and an estimate of the confidence intervals, or rather the credibility interval, given the data.

This Bayesian learning is iterative and sequential, so that the result of one Bayesian inference can form the prior of another, i.e. it is an additive process (Kruschke, 2015, p. 17). Moreover, at the conceptual level, this allows different sources of information to be combined (Bryant and Zhang, 2018, pp. 219–224). This enables that they can be mapped to the same set and the same real-world domain, e.g. probabilities. This fact has long been exploited by archaeology in using stratigraphic information to make radiometric dating more accurate (Ramsey, 1995). ^{14}C dates and stratigraphy are something completely different, but both can be mapped to the probability of older and younger and combined in this way. The same is also feasible when it comes to the probability of population sizes or population densities or their derived dynamics.

A further characteristic of Bayesian modeling is that, due to the fact that results of a Bayesian inference can be regarded as a prior for the next one, a hierarchical formulation of problem domains is possible. Parameters

that are necessary for an estimation, such as the relationship of population density to the deforestation signal in pollen data, need not be specified explicitly, but can be given by probability distributions and then estimated in the model itself (Bryant and Zhang, 2018, p. 186). The more data available, the more degrees of freedom can be estimated with a reasonable loss of confidence or a reasonable width of credibility intervals (Kruschke, 2015, p. 112). For the estimation of these parameters, in turn, submodels have to be created which describe the relationship of the data to the characteristics of the parameter. This can be carried out over several levels, depending on necessity (Kruschke, 2015, pp. 221–222).

3 Materials: Population proxy data

The case study area north of the Swiss Alps (Figure 1) covers about one third of Switzerland’s territory and comprises the partly flat, but largely hilly area, between the Jura Mountains and the Alps. It averages an altitude of between 400 and 600 m a.s.l. It is a favourable area for settlement and agriculture and especially the Swiss Plateau is by far the most densely populated region of the Switzerland today. The Swiss Plateau between Lake Zurich and Lake Geneva will serve as a core region in our case study, because archaeological data from there is most abundant and accessible. Although it is a basin, depending on the region it has a very diverse natural landscape: shaped by glaciers during the ice ages, the many lakes and bogs that characterise the landscape today also provide excellent preservation conditions for the numerous Neolithic and Bronze Age lakeside settlements, as well as a rich pool of sources for vegetation reconstructions by means of pollen analyses. Thanks to the very active and efficient archaeological research and heritage management there is an abundance of archaeological information, including known sites as well as dendrochronological and ^{14}C data.

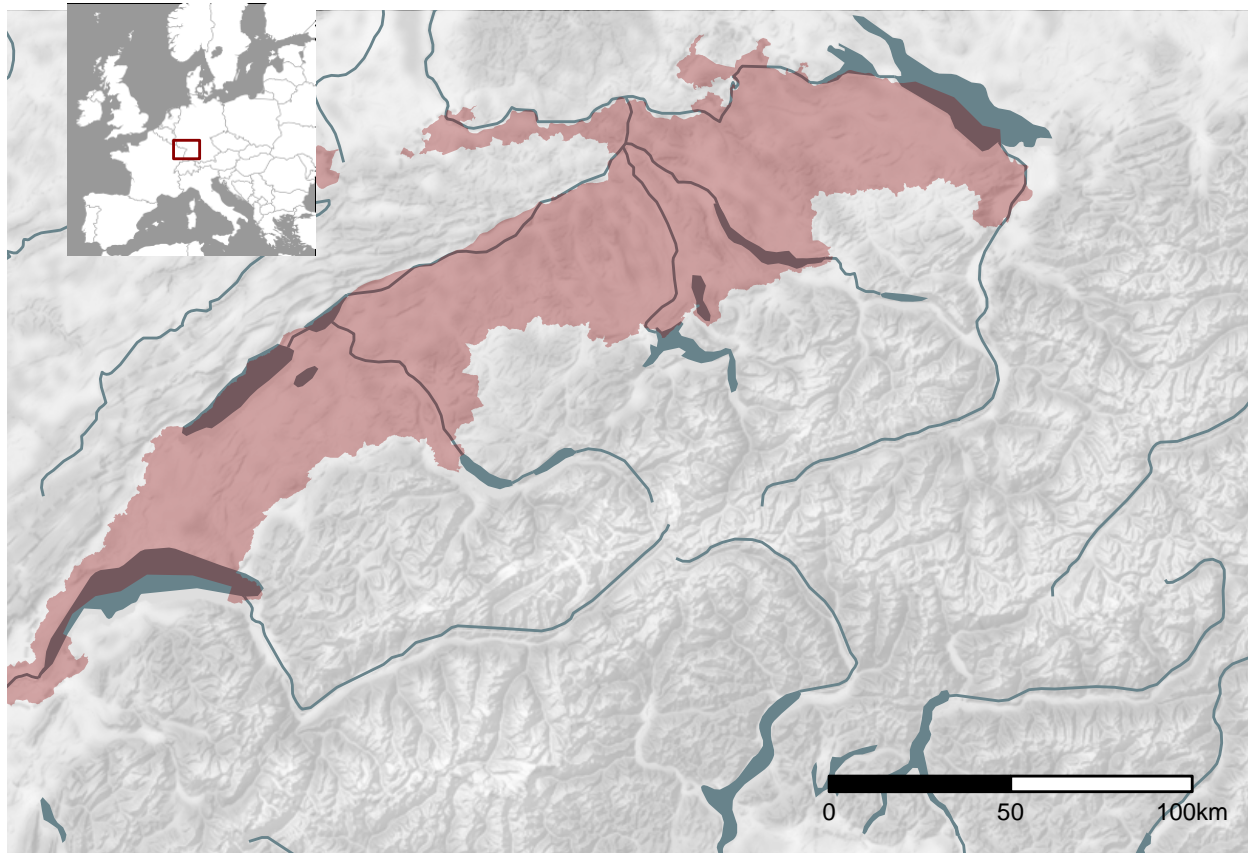


Figure 1: Location and extent of the Swiss Plateau as biogeographical region (based on swisstopo) including additional low altitude areas in the north of Switzerland (regions along the High Rhine between Schaffhausen and Basel).

Our case study targets the period between 7000–1000 BCE. The lower limit of this window was chosen to avoid the so-called ‘Hallstatt plateau’ on the Northern Hemisphere radiocarbon calibration curve, which would cause difficulties for the ^{14}C proxy data. The upper limit was chosen to coincide with post-glacial changes in pollen spectra, before which the openness indicator is highly unlikely to reflect human influence before 7000 in the working area.

In principle, a large number of different data sources can be integrated into the overall model as proxies, provided that these observations a) can be understood as dependent on the population density in the past, and b) a model-like description of this dependence can be created. Table 1 provides a non-exhaustive list. For our case study, we used: a landscape openness indicator; an aoristic sum of sites based on typological dating; a sum calibration; and frequency data for dendro-dated lakeshore settlements in the Three Lakes region (western Swiss Plateau).

Table 1: A incomplete list of possible observation that can be linked to population developments in the past. Proxies used in this study are highlighted.

Proxies
Expert estimates
Ethnographic Analogies
Carrying Capacity
Economic modelling
Extrapolation of buried individuals
Burial anthropology
Settlement data, number of houses
Settlement data, settlement size
Aoristic analysis
Dendro dates
Amount of archaeological objects
Radiocarbon sum calibration
Estimates based on specific object types
Human impact from pollen or colluvial data
aDNA based estimates
...

3.1 Dendro-dated lakeshore settlements

With the vast areas of arable soils with small slope gradient compared to the Jura and the Alps, and a dense network of water bodies, the Swiss Plateau has always been a particularly favourable area for human settlement in Switzerland. From the Neolithic onwards, settlement areas were concentrated along its rivers and lakes (Christian Lüthi, 2009). Thus, our working region offers on the one hand excellent data for demographic estimation, but on the other hand poses very specific problems for such an undertaking. If we have high-resolution information on the temporal sequence of individual settlements at the lakeside settlements by means of dendro data, this also might cause a research problem with regard to the ^{14}C data often used as a proxy.

The dataset we use for the number of dendro-dated wetland settlements in the Three Lakes region was collected by Julian Laabs for his PhD thesis (Laabs, 2019). Details on the creation of this data series will be published at the referenced location. The time series used here runs from 3900 to 800 BCE, and contains the number of chronologically registered fell phases at individual settlements. This results in a time series that reflects the settlement of the lakeshores in the Neolithic and Bronze Age periods.

3.2 Summed radiocarbon

The dataset for the ^{14}C sum calibration primarily consists of data from the XRONOS database (<https://xronos.ch>), supplemented by dates from the unpublished PhD thesis of Julian Laabs (Laabs, 2019) and the data collection of (Martínez-Grau et al., 2021). It contains a total of 1135 single ^{14}C data from 246 sites. The dates were selected so that their distribution area coincides with the catchment area of the pollen proxy (see also Figure 2). The dates in the dataset range in ^{14}C years from 10730 to 235 uncal BP. This time window extends beyond the study horizon in order to minimise boundary effects.

We binned the data at site levels to obtain a temporally dispersed count and thus an expected value of contemporaneous ^{14}C dated sites. For the creation of the cumulative calibration, the corresponding functions of the R package rcarbon (Crema and Bevan, 2021) were used with their default settings.

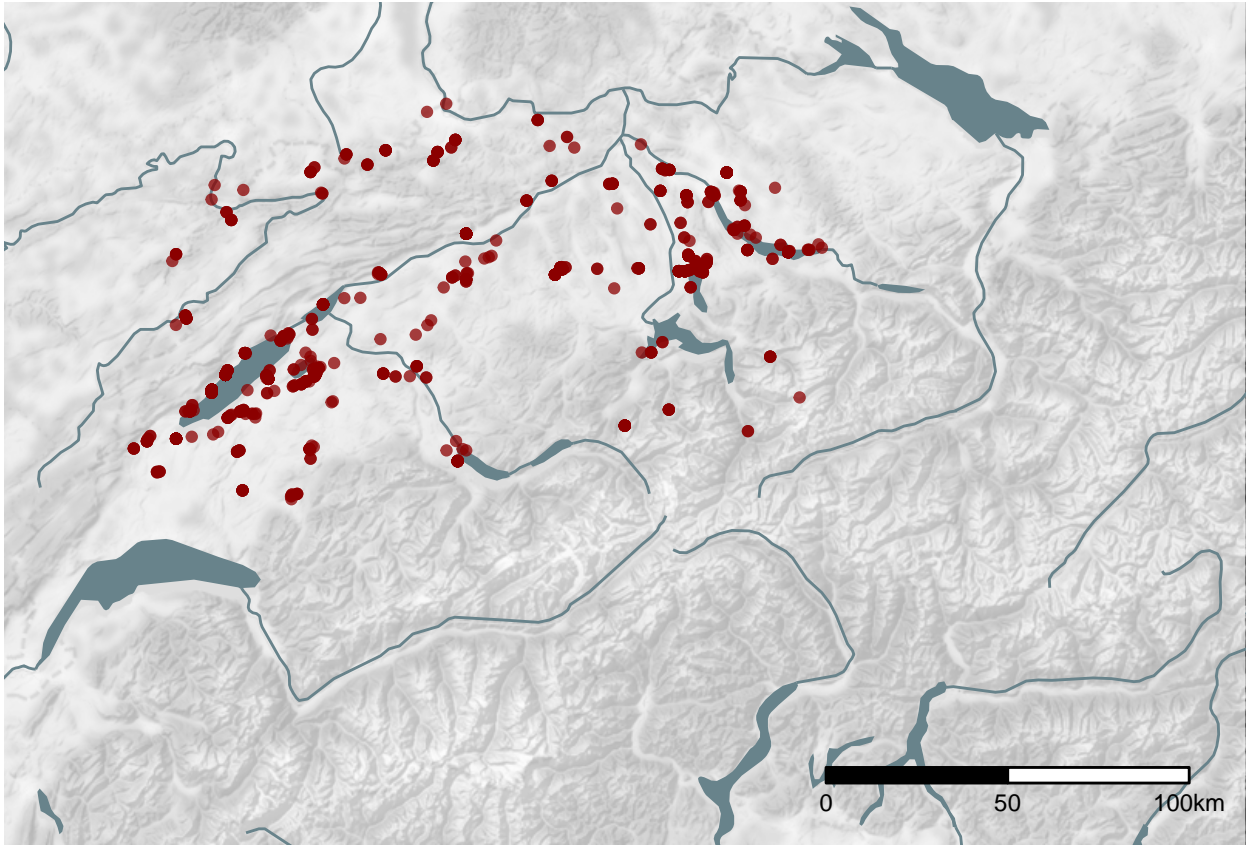


Figure 2: The location of the ^{14}C dated sites in the dataset.

We can now compare these two data sets (Figure 3). In fact, there is a not uninteresting fit between the two data series. However, it must be assumed that the two dating methods, even if they would contradict each other, actually complement each other, and thus allow a better overall unified picture of the actual settlement density than each of the individual proxies would allow on their own.

3.3 Aoristic sum

To add another archaeological indicator of occupation, we include relative dating information obtained from the Swiss cantonal archaeology/heritage management authorities (Figure 4). These are primarily derived from scattered surface finds, which often have a low dating accuracy. We incorporate this data into our model as a typologically dated aorist time series. The dating accuracy is only in the range of archaeological periods, but the advantage is that we are not bound to the conditions and problems of radiocarbon dating and thus methodological issues of sum calibration can be avoided. Furthermore, this data provides an independent

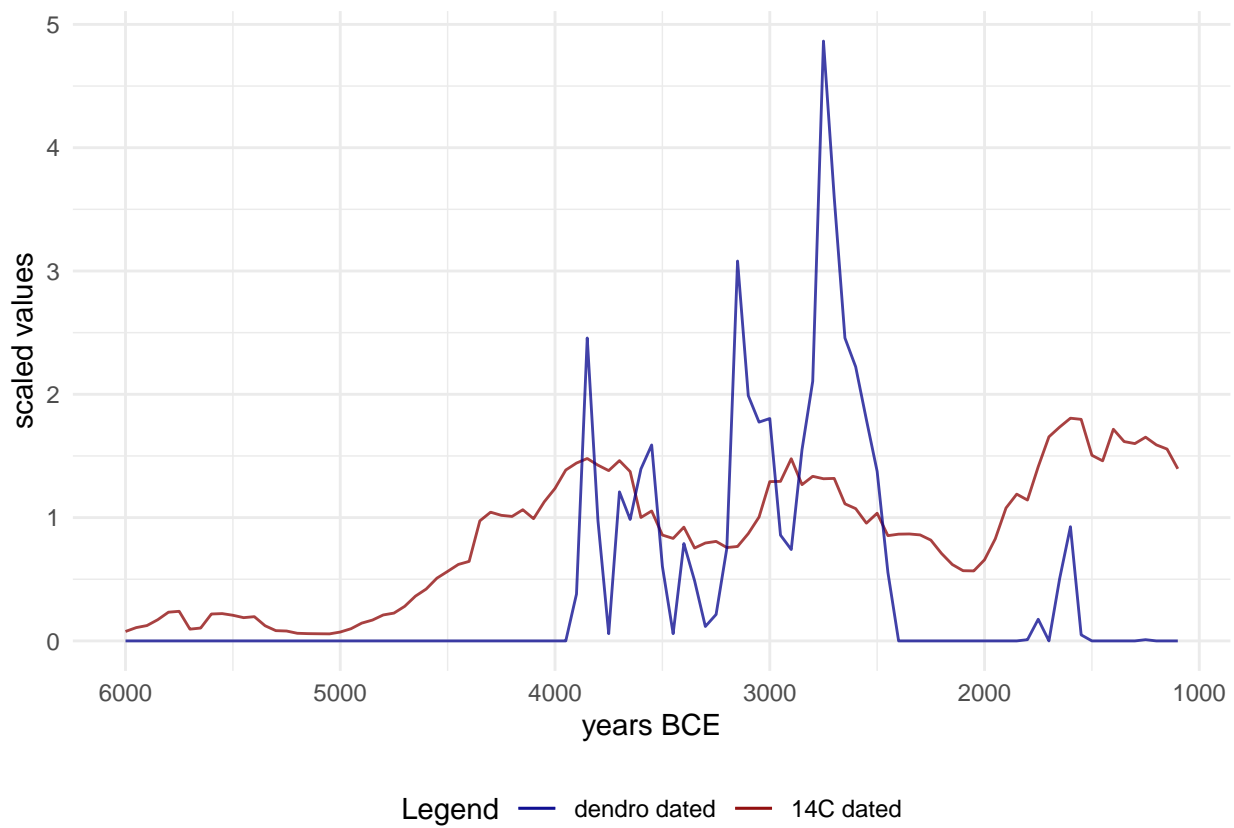


Figure 3: Comparison of the scaled (non-centered z-transformed) number of ^{14}C and dendro-dated sites over time in the dataset used.

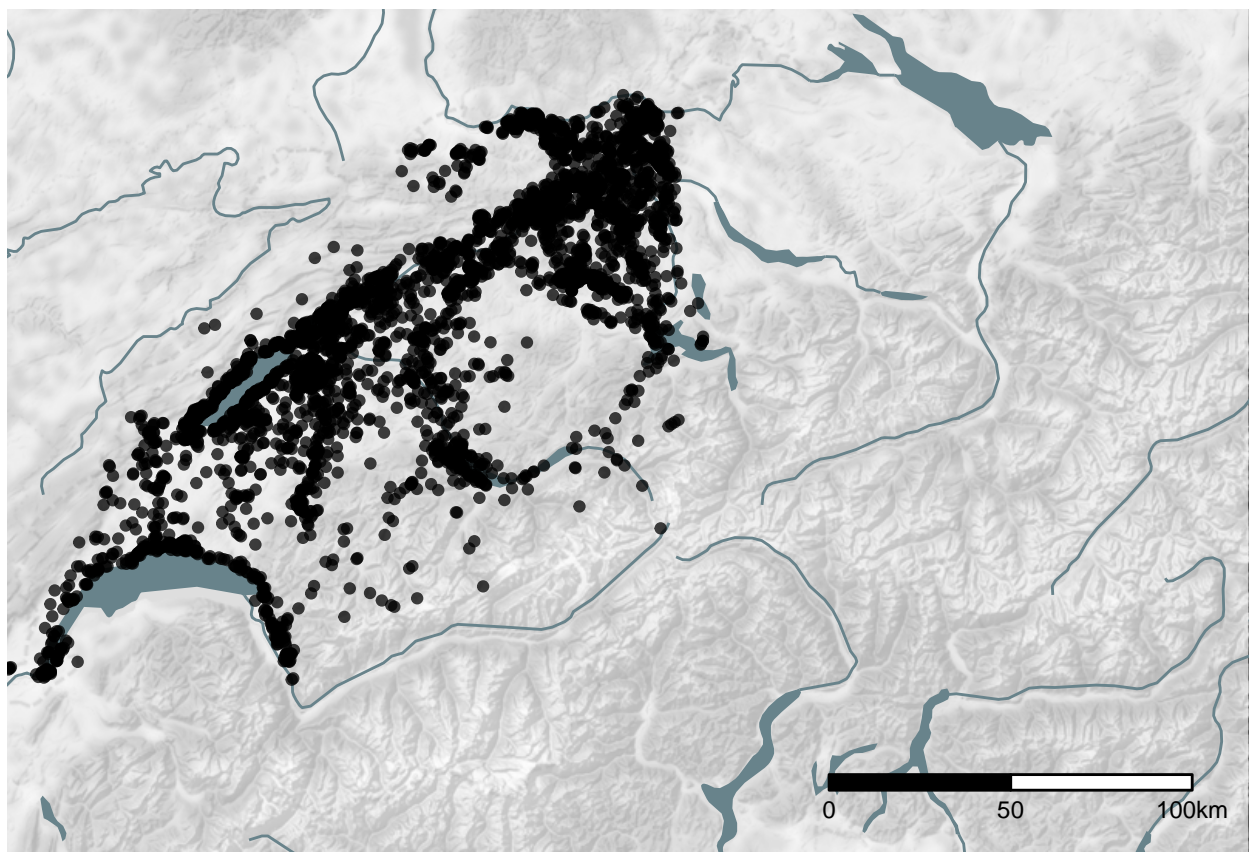


Figure 4: The location of the sites from the find reports of the cantonal archaeology (heritage management). The locations are ‘fuzzed’ by ~1km.

indicator with regard to the methodology of the ^{14}C data, even if they are influenced by similar transmission filters and archaeological conditions as the evaluation of ^{14}C data. Data from 4321 sites were included in the aoristic sum, which is a very rough indicator due to the low dating accuracy offered by archaeological phases, but which nevertheless has an important role in the normalisation of the data due to its independence from calibration effects.

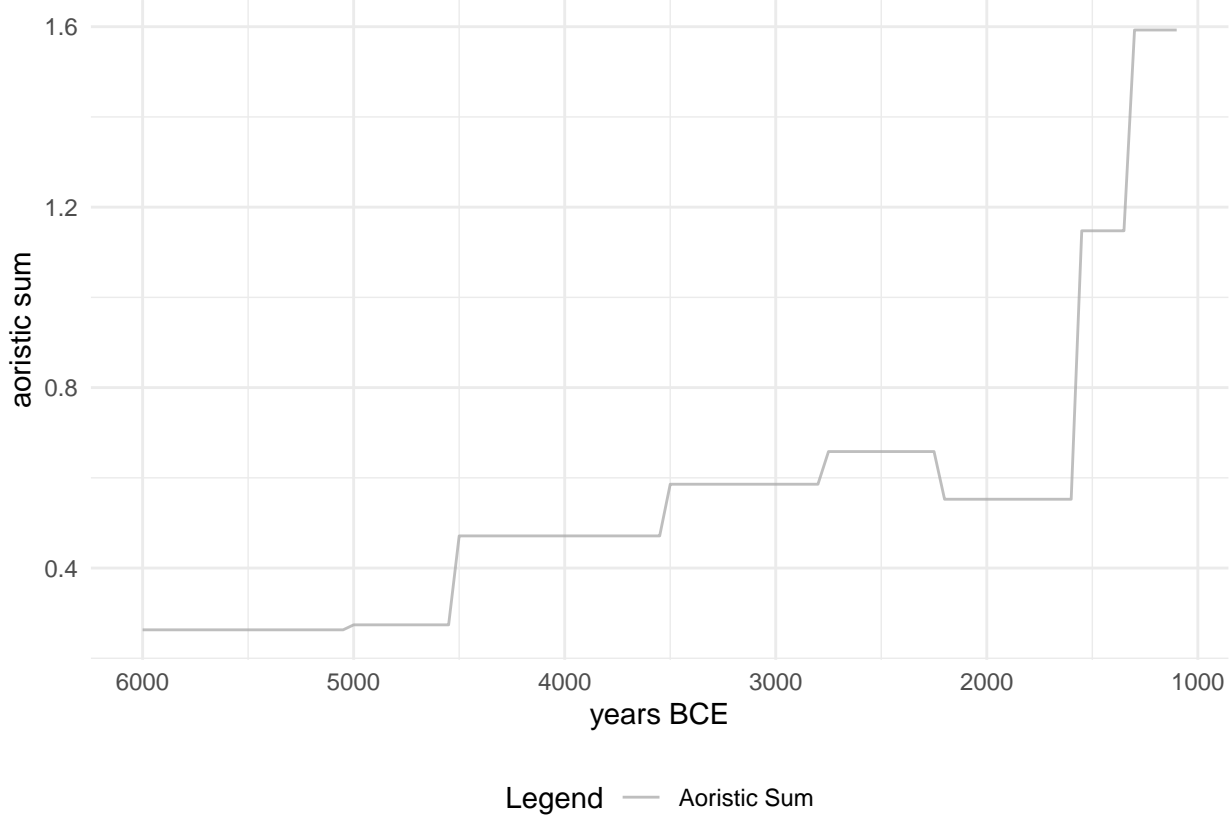


Figure 5: Aoristic sum of the archaeological sites used in this analysis.

3.4 Landscape openness

The natural conditions of the lakes of the Swiss Plateau enable not only highly precise dating of archaeological sites, but also a very dense network of pollen analysis. We make use of this fact by generating a supra-regional openness indicator for the vegetation from the pollen data (Figure 6). This proxy has the specific advantage that it is not dependent on preservation conditions, as archaeological indicators are. This makes it particularly valuable for indicating or compensating for systematic distortions that result from temporally specific settlement patterns and archaeological preservation conditions.

The utilisation of this proxy is based on the assumption that the higher the population density in an area, the greater the human influence on the natural environment (Lechterbeck et al., 2014), and that the extensiveness of agricultural activity in an area is related to human population density (Zimmermann, 2004). Evidence of land clearance in pollen diagrams can therefore provide further indications of population dynamics where humans can be assumed to be the main driver of this process, which is the case in much of Europe. The full procedure for deriving this proxy from several different pollen diagrams is detailed in a previous publication (Heitz et al., 2021). In this study, five pollen diagrams from sites mainly in the hinterland of the large Alpine lakes were used. The technical steps are also documented in the accompanying R compendium. The percentage pollen data, based on a pollen sum of all terrestrial taxa of the individual sites, was combined into one data set by means of a principal component analysis (Figure 7). Only terrestrial pollen taxa with a frequency of more than one third and, if present, with an average frequency of at least 0.1% were

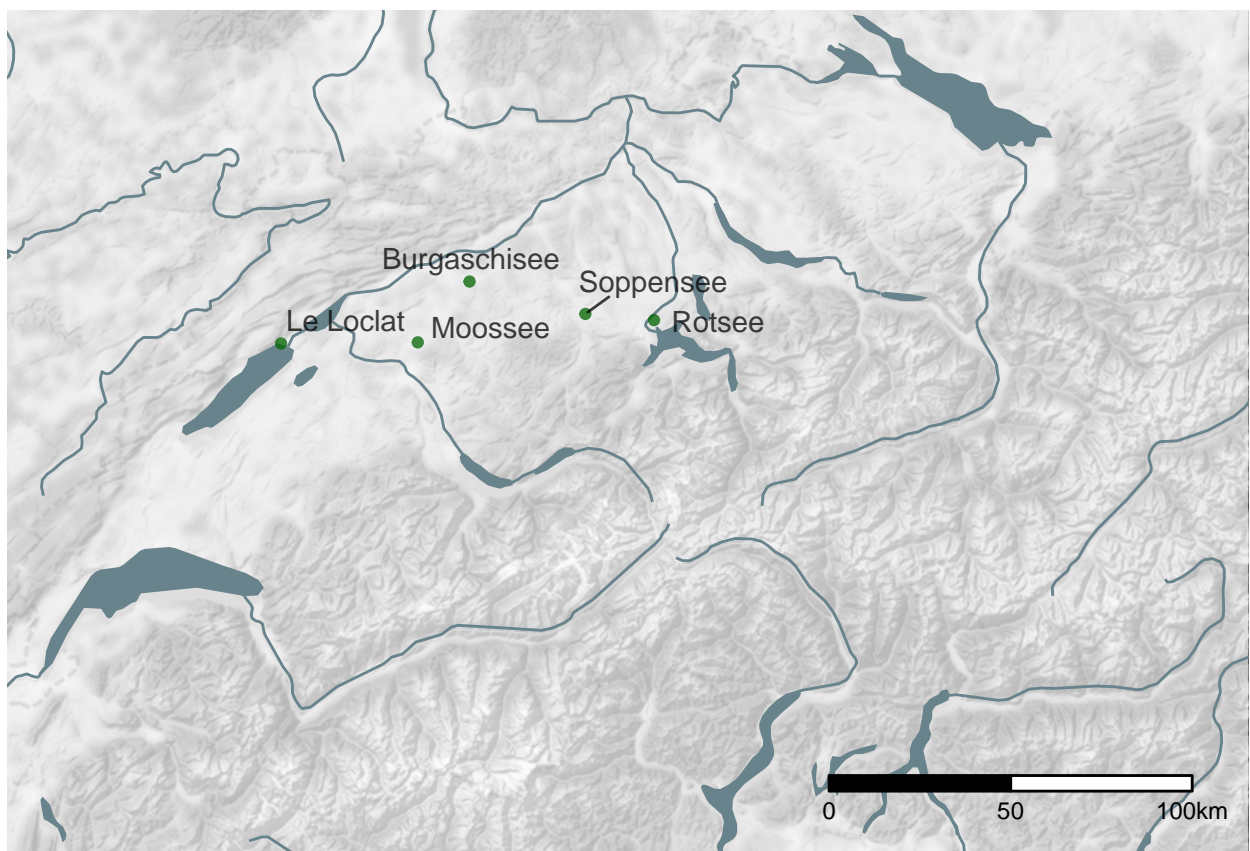


Figure 6: Location of the pollen profiles used for the openness indicator.

selected to reduce potential disturbance by rare species. Cereal pollen was explicitly retained as an important anthropogenic indicator. As each sample is absolutely dated, the data on the x-axis can be plotted against the openness value on the y-axis to obtain a time series time series for land clearance.

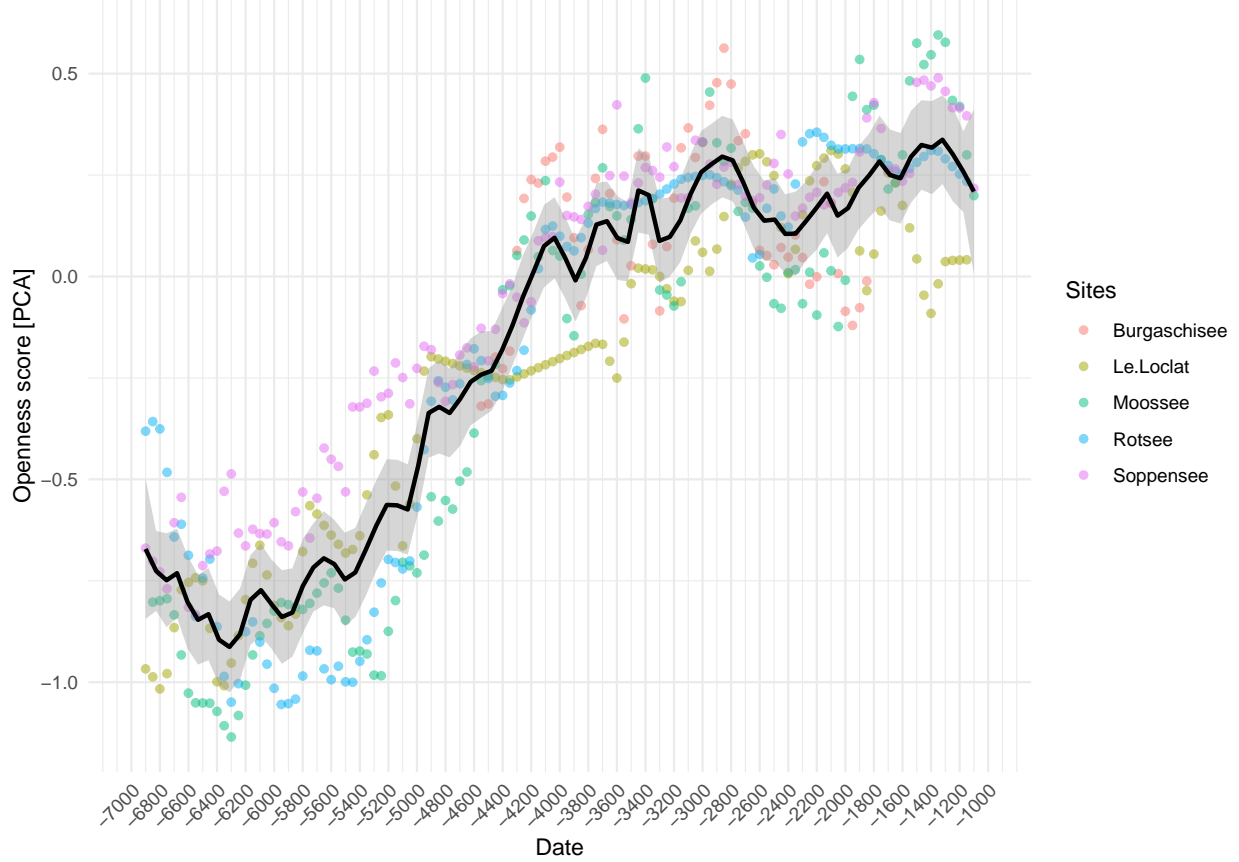


Figure 7: Value on the first dimension of the PCA against dating of the samples for the individual pollen profiles and their combined average value as the openness indicator.

3.5 Other proxies

Unfortunately, there is no burial data available in the case study area that could be usefully incorporated into such this model due to the absence of regular burials for larger parts of prehistory. Formation conditions, in this case most likely C-transformation (Schiffer, 1987), the active cultural choice to not use archaeological traceable burial practices, prevent their use in this study. Nevertheless, we see a very high potential for other regions in the integration of demographic indicators from burial data in order to enlarge the canon of methods and the range of proxies.

4 Methods: Bayesian model

The sum calibration, openness and the dendro-dated settlement data was smoothed by means of a moving average with a window of 50 years. The aoristic sum was not smoothed, because it already has a very coarse temporal resolution. The range of the smoothing window corresponded to the sample interval, with which a unified resolution of 50 years was obtained for all proxies as time slices for the model. In addition, all data was restricted to the window of observation of 7000–1000 BCE.

In the construction of our ‘observational model’, we considered all these proxies as informative of the number

of settlements located in the north of the Swiss Alps. Consequently, we shift the causality and consideration of measurement error, which is certainly inherent in each of these proxies, to a preceding ‘process model’, in which a Poisson process describes the number of simultaneous settlements. In doing so, we establish a likelihood that estimates how credible the data is, given the model.

4.1 Process model

A special class of Bayesian hierarchical models are so-called State Space Models (also known as Hidden Markov Models). These are specifically designed for time series and follow two basic principles. First, a hidden or latent process is assumed, which represents the state of the variable of interest x_t through the entire time series. Over time, it is assumed that every state of variable x in the future, as well as in the past, is bound by a Markov process to the state of variable x at time t . At the same time, it is assumed that certain observations, represented in variable y , are dependent on the state of variable x at time t . This means that there is a relationship between the variable x and the state of variable y over time. This implies that a relationship between the individual states of variable y is generated over time via the hidden variable x , which itself is not observable.

This basic structure of this class of model makes it particularly useful and suitable for the purpose of demographic reconstruction using archaeological and other data which are reflective of population density in the past. This population density itself is not accessible or measurable by our means. All we have at our disposal are observations derived by unknown transfer functions. These can be of very different natures, such as number of archaeologically observable settlements, or other effects that can be observed through time series, and which are influenced by population in a given area. In our case study, these are the openness indicators from pollen data, which we can interpret primarily in terms of human influence and its intensity. On a more abstract level, we could also include expert estimates, as these also happen on (often unspecified) bases that are at least indirectly influenced by past population density.

The overall model for the estimation of demographic developments is broken down into several hierarchically interconnected individual elements in accordance with the basic structure of a state space model. The basis is a process model that represents the demographic development itself in terms of a structure model, without this model already being explicitly configured with data.

In this process model we assume that the latent variable ‘number of sites’ is strongly autocorrelated across different time periods, i.e. the number of sites in 3000 BCE is strongly conditioned by the number of sites in 3050 BCE, and so on. In principle, one can represent a population development in such a way that the population at time t results from the population at time $t - 1$ times a parameter λ , which represents the population change at this time. This gives us the basic formula:

$$N_t = N_{t-1} * \lambda_t$$

The Poisson distribution is particularly suitable for modelling frequencies. It is a univariate discrete probability distribution that can be used to model the number of events that occur independently of each other at a constant mean rate in a fixed time interval or spatial area. It is determined by a real parameter $\lambda > 0$, which describes the expected value and simultaneously the variance of the distribution. Thus, the relationship shown above can also be rearranged as follows:

$$\begin{aligned} N_t &\sim dpois(\lambda_t) \\ \lambda_t &= N_t \end{aligned}$$

If we now have information about the change in population development (the proxies), we can use this to enter it into the model via a change in λ . This is done in the form of a regression: for all proxy values—represented as a vector of independent variables $x \in R^n$, with R^n as an n -dimensional Euclidean space, described in this case by the n dimensions of the n variables—then the model takes the form:

$$\log(E(Y | x)) = \alpha + \beta'x$$

Using the logarithm as a link function ensures that λ , which must always be positive for a Poisson process, can also be described by variables (proxies) that range in the space of real numbers and can therefore also be negative. β can serve here as a slope factor, just as in a normal linear regression. In our case, it functions as a scaling factor for the individual proxies. α , is to be understood as an intercept. If there were no change due to the variables, the regression would fall back to this value. This corresponds to the desired behaviour. In the case of population trends, the intercept would be equal to the value of the population in the previous time period, plus or minus the changes resulting from the variables. If there is no change from these variables, then λ , and thus the expected value for the current time step would be equal to that from the previous time step:

$$\log(\lambda_t) = \log(N_{t-1}) + \sum_{i=1}^n \beta_i x_{t,i}$$

Since λ and N are essentially in the same range (e.g. if *lambda* = 1, the expected value for N would also be 1), N_{t-1} must also be log-transformed in the above formula to obtain the congruence of both values. The values for population size N_t as well as for population change λ_t are time-dependent. At each individual point in time in the time series, these variables can or will also take on different values. However, we can narrow down the structure of population change even further. We can assume that, considered overall over time, the population change will not exceed certain limits over the entire timespan, though it is not possible to specify this at this point.

Thus, we can define the limits, the *max_change_rate* as a time independent variable, again without specifying them with fixed values at this stage. The estimation of these parameters for the entire model, as well as the estimation of the respective population change per time section, results from the modelling and the interaction with the data, respectively. Overall, this represents a hierarchical model that can be noted as follows:

$$\begin{aligned} \text{max_growth_rate} &\sim \text{dgamma}(\text{shape} = 5, \text{scale} = 0.05) \\ N_t/N_{t-1} &< (\text{max_growth_rate} + 1) \\ N_{t-1}/N_t &< (\text{max_growth_rate} + 1) \end{aligned}$$

The gamma distribution used centres the probability in a range [0, 1[, adding 1 makes this range [1 – 2[. This prevents the number of sites from explosively increasing between two time periods, which would be unrealistic given our sampling interval (50 years), and would lead to problems for the convergence of the model. The interaction of these parameters results in the following prior probability distribution for λ and thus the growth (or change) rate of the population.

4.2 Observational model

During the development of our model, we experimented with but ultimately abandoned the idea of implementing dedicated observation models adapted to the conditions of the individual proxies and their generating processes. We found that underdetermination of currently usable data in the model, having many degrees of freedom, produced a high degree of equifinality in the solutions and thus led to a high path dependency in individual model runs. As a result, it was almost impossible to achieve convergence of the overall model. Nevertheless, we believe that in future applications of the model with more data, a larger geographical coverage and/or, especially, a regionalised approach with information transfer by means of partial pooling, this more specific approach would be a feasible and a very useful approach.

The implementation we present in this paper instead represents a Poisson regression, where the proxies are used to inform the change in the number of settlements from time step to time step. For this purpose, the individual proxies were z-normalised. The absolute differences from one time step to another were then

computed from the resulting time series. Thus, if the value of the proxy increases, this results in a positive difference from the previous time step, and vice versa.

$$z_t = \frac{x_t - \bar{x}}{\sigma_x} \mid \sigma_x := \text{Standard Deviation}$$

$$\delta z_t = z_t - z_{t-1}$$

The sum of the resulting differences between the time steps, together with the settlement number of the previous step as the expected value, then forms λ_t as the expected value for the settlement number of the current time step.

$$\log(\lambda_t) = \log(N_{t-1}) + \sum_{i=1}^n \beta_i \delta z_{i,t}$$

Here, β_i is a scaling factor that represents the influence of the respective proxy. It is a confidence value of the model for the respective proxy, so that the sum of all β_i results in 1.

$$\sum_{i=1}^n \beta_i = 1$$

A probability distribution that can be used for this purpose in a hierarchical Bayesian model is the Dirichlet distribution, which is a multivariate generalization of the beta distribution, commonly used as prior distributions in Bayesian statistics. Its density function gives the probabilities of i different exclusive events. It has a parameter vector $\alpha = (\alpha_1, \dots, \alpha_n) \mid (\alpha_1, \dots, \alpha_n) > 0$, for which we have chosen a weakly informative log-normal prior. The priors for the log-normal distribution in turn come from a weakly informative exponential distribution for the mean and a log-normal distribution with μ of 1 and σ_{\log} of 0.1:

$$\begin{aligned} \beta_i &\sim \text{Dir}(\alpha_{1-i}) \\ \alpha_i &\sim \text{LogNormal}(\mu_{\text{alpha}_i}, \sigma_{\text{alpha}_i}) \\ \mu_{\text{alpha}_i} &\sim \text{Exp}(1) \\ \sigma_{\text{alpha}_i} &\sim \text{LogNormal}(1, 0.1) \end{aligned}$$

As an intuition, this means that we consider the sum of the proxies as determinant for the number of settlements. The estimation therefore assumes that all proxies together give the best possible estimation result for contemporaneous sites at time t, whereby the share of each individual proxy is considered variable and is estimated within the model. This share is recorded within the model as the parameter p.

The error value is represented by the Poisson process in the process model, rather than directly as an estimation error for the individual proxies. Thus, our model does not correspond to a classical state space model, where the measured values are each considered to be error-prone. In the implementation, the model finds the best possible combination or compromise between the individual proxies to describe a settlement dynamic that is given by them. In addition, the number of sites is converted into population density using some (certainly debatable) parameters that we have defined but which are only scaling factors for the intermediate value of number of settlements. For this, we assume that each site represents a number of people that is poisson distributed around the value 50. The number 50 represents a compromise, as both Mesolithic and Neolithic and Bronze Age settlement communities need to be represented. By means of a data series, which would represent an evidence-based estimate of the temporal development of settlement sizes, this specification could be made based on data. From the number of sites and the mean number of individuals represented in each case, a population density can be calculated using the case study area (12649 km²). The estimated result of the model is thus comparable with estimates from other sources or the literature.

In earlier implementations, expert estimates were also integrated into the model. However, since these are highly contradictory for the working area (Figure 8, we found they had little influence on the model and also

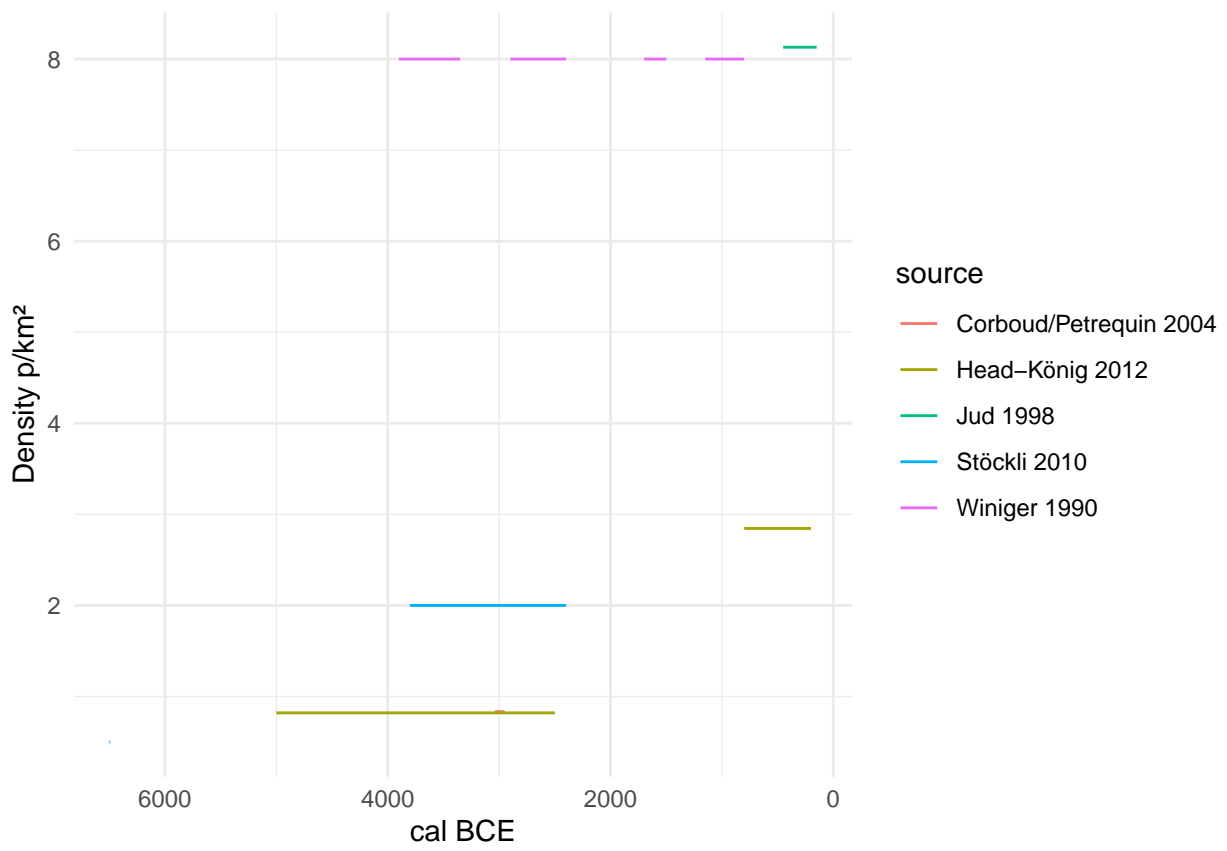


Figure 8: Expert estimations for the population density on the Swiss Plateau from different authors.

significantly increased its runtime. We therefore excluded them in the implementation presented here, but again, given a larger geographical range and thus a higher information density, this proxy could be usefully integrated into future applications.

4.3 Model fitting

The model was fitted using the R package *nimble* (version 0.11.1, R version 4.1.3). For this purpose, 4 chains were run in parallel. Achieving and ensuring convergence and sufficient effective samples (10000) for a reliable assessment of the highest posterior density interval was carried out in steps.

In a first run, the model was initialised for each chain and run for 100000 iterations (with a thinning of 10). On a reasonably capable computer (Linux, Intel(R) Xeon(R) CPU E3-1240 v5 @ 3.50GHz, 4 cores, 8 threads), this takes approximately a minute.

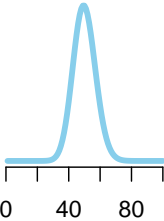
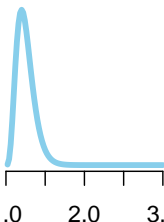
In a second step, the run was extended until convergence could be determined using Gelman and Rubin's convergence diagnostic, the criterion being that a potential scale reduction factor of less than 1.1 was achieved for all monitored variables. Convergence occurred after about thirty seconds.

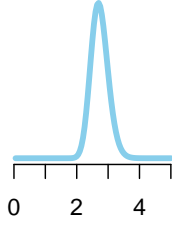
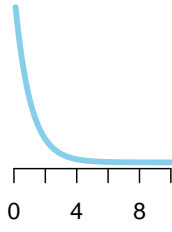
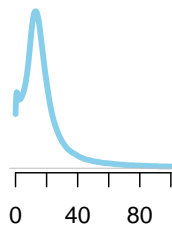
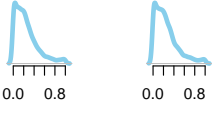
Due to the high correlation of the parameters and thus a low sampling efficiency, the collection of at least 10,000 effective samples for all parameters in the third step took about five hours.

For the fitting process, a starting value of 5 p/km² for a population density of the Late Bronze Age (1000 BCE) was taken from the literature, which may represent a general average value for all prehistoric population estimates (Nikulka, 2016, p. 258). For the model, this was set as the mean of a normal distribution with a standard deviation of 0.5, which should give enough leeway for deviations resulting from the data. Nevertheless, especially the late part of the reconstruction is of course clearly influenced by this predefined value.

For the traceplots and the prior-posterior overlap as well as the density functions of the posterior samples of the individual parameters, please refer to the supplementary material.

Table 2: Priors and fixed parameters used in the model.

Priors	Value	Plot/Comment
MeanSiteSize	dpois(50)	 A density plot showing a single sharp peak centered around 50. The x-axis ranges from 0 to 100 with major ticks at 0, 40, 80.
max_growth_rate	dgamma(shape = 5, scale=0.05) + 1	 A density plot showing a single sharp peak centered around 1.5. The x-axis ranges from 1.0 to 3.0 with major ticks at 1.0, 2.0, 3.0.

Priors	Value	Plot/Comment
mu_alpha	dlnorm(1,sdlog=0.1)	
a_alpha	dexp(1)	
alpha	dlnorm(mu_alpha[j],sdlog=a_alpha[j])	
p	ddirch(alpha[1:4])	
Parameters		
nEnd	5	
AreaSwissPlateau	12649 km ²	
Initial Values		
lambda _{1:nYears}	$\log(1 - 10^{\frac{1}{nYears-1}})$	exponential increase of the factor 10
PopDens _{1:nYears}	nEnd (=5)	
nSites _{1:nYears}	50	

5 Results

The population density estimated by the model (Figure 9) ranges on between 0.2 p/km² for the beginning of the estimate (6000 BCE) and 4.8 p/km² for the end of the estimate (1000 BCE), reaching a maximum of 6.5 p/km² for the time slice 1250 BCE. Thus, the estimate remains within the values that are also considered plausible by the expert estimates. Clear peaks are reached around 1250 BCE, as well as around 2750 BCE,

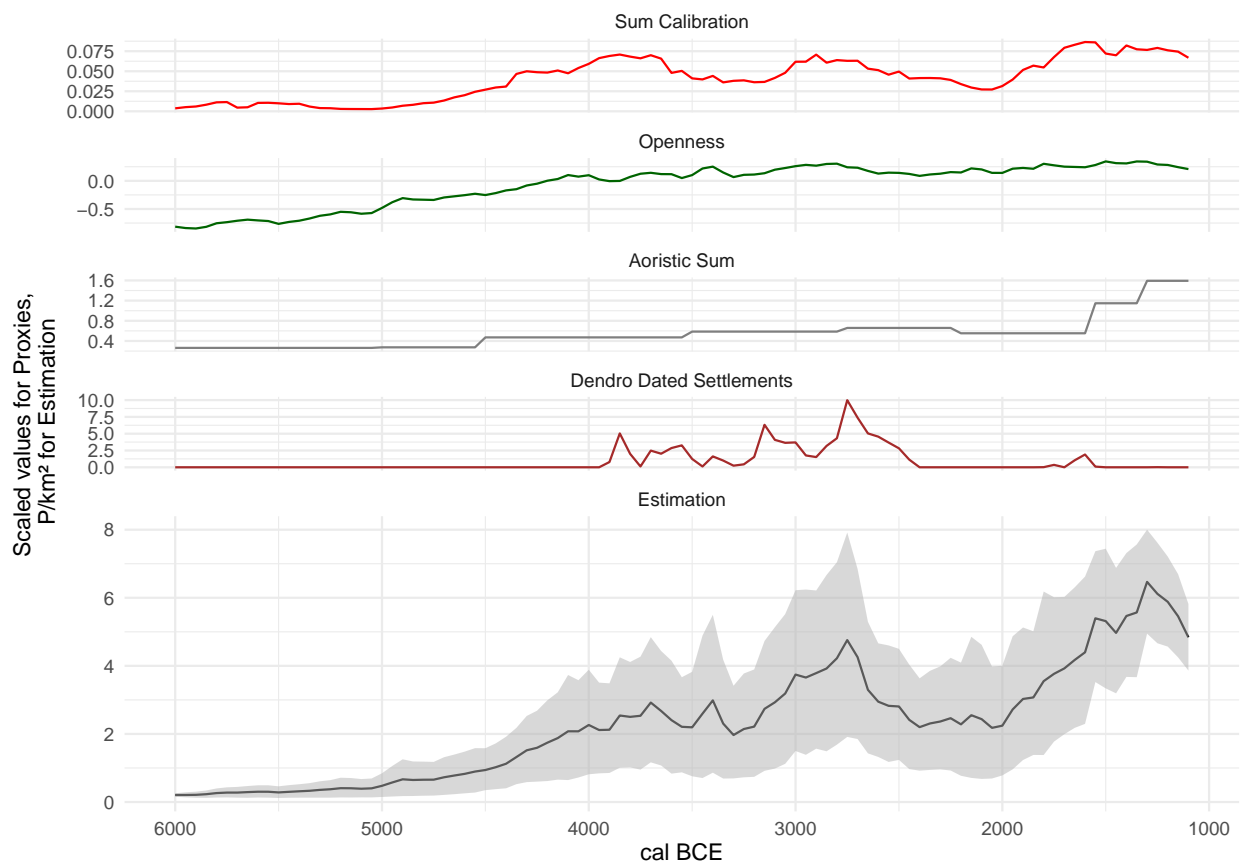


Figure 9: The estimate of the population density resulting from the model and the four proxies, which are also plotted (scaled) for comparison.

which corresponds to the transition to a ceramic style as observed for sites of the Swiss Plateau influence by the Corded Ware ceramic style (Hafner, 2004).

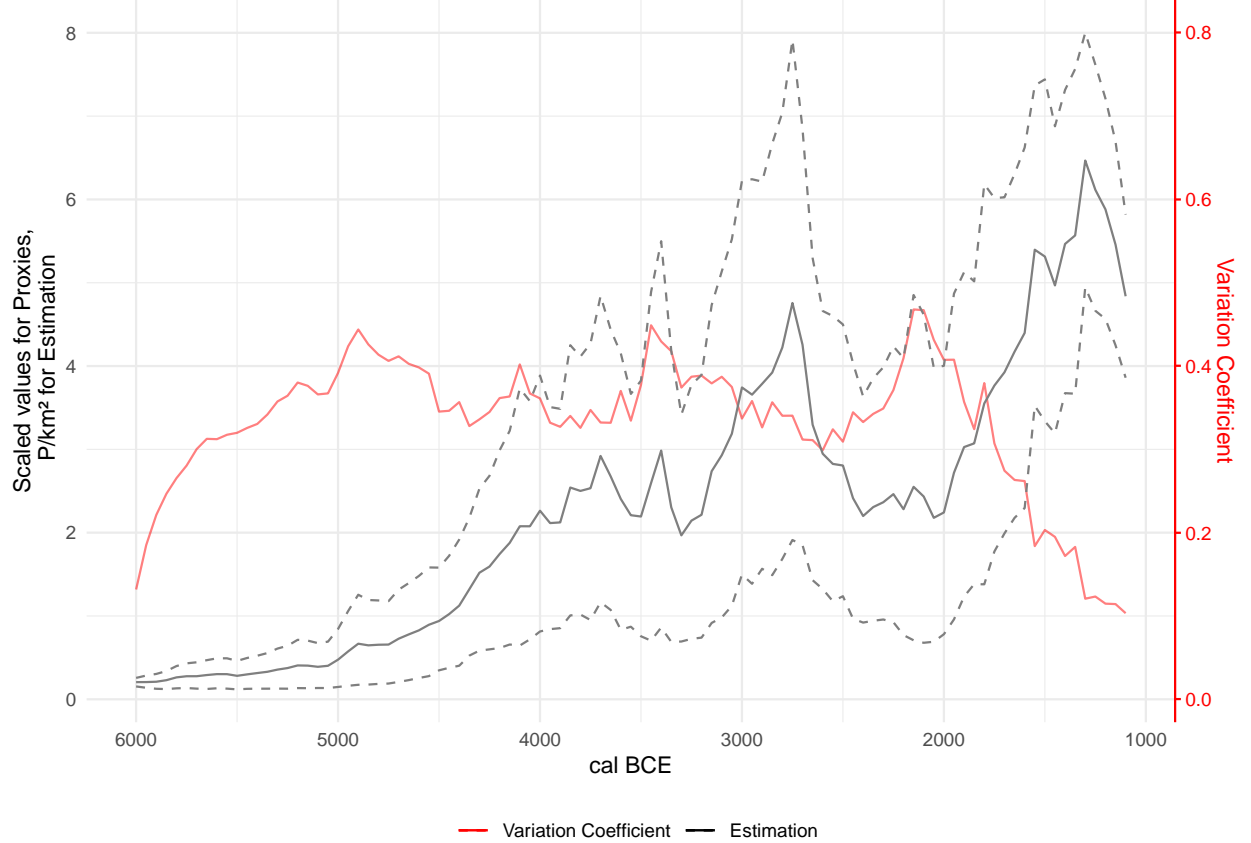


Figure 10: The variability of the estimate of the population density over time, with the estimate itself for reference.

The temporal distribution of the variability in the estimate (Figure 10) allows us to assess at which time steps the model attempts a more accurate estimate, and at which the uncertainty is greater due to e.g. contradictions in the proxies. The coefficient of variation is 0.13 for the beginning and 0.1 for the end of the estimate, the greatest variability is reached around 2150 BCE with 0.47. This is not astonishing as there are fewer archaeological contexts recorded connected to the earlier phase of the Early Bronze Age c. 2200-1800 BCE, this picture changes from c. 1800 BCE onwards David-Elbiali (2000). The beginning and end of the time series are relatively clearly determined. The end results from the *a priori* setting of the parameter, but also here, as at the beginning of the series, the proxies are very uniform, which explains the low variability. Overall, the variability is relatively uniform over the entire course of the estimation and averages over all time slices at 33% of the respective mean.

Within the model, the parameter p was estimated, which reflects the relative weight given to the individual proxies used in the estimation of the number of settlements. This parameter is variable, but has only a scaling influence on the final estimate of population density.

By looking at the distribution of posterior samples for the share of each proxy (Figure 11), it is clear that the model weights the openness indicator the highest. The average is slightly above 60%. The next most important indicator is the sum calibration value, which has an average of about 20%. The aoristic sum is slightly above 10%, whereas the importance of the dendro-dated settlements is below 10%. The reason for the latter is certainly that there are no lakeshore settlements over large areas of the time window, and therefore the proxy achieves a low confidence value in comparison with the other estimators. In the case of the aoristic

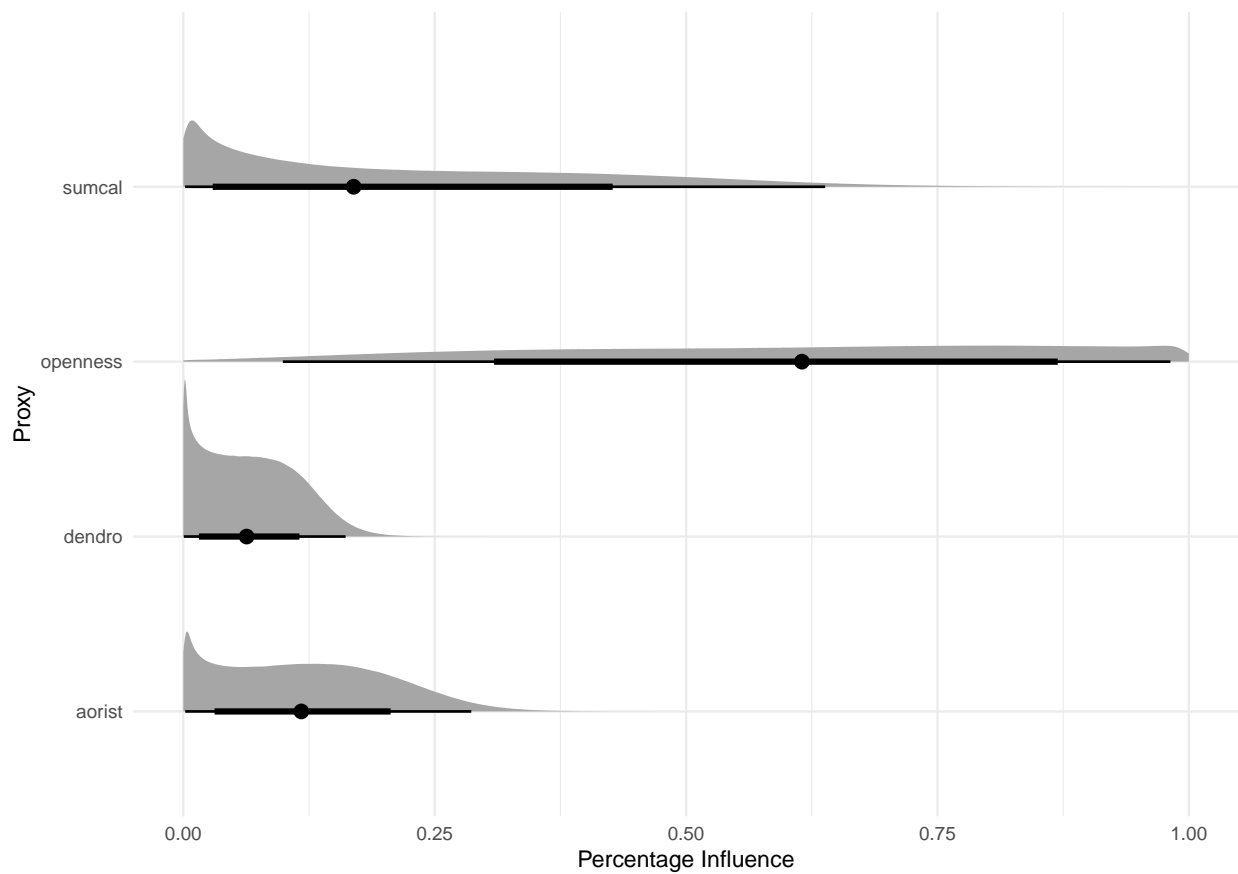


Figure 11: Distribution of the influence ratio of the different proxies on the final estimation of the number of sites.

sum, it is certainly the fact that it is flat over large sections and has little structure, making it difficult to relate to the other estimators. The sum calibration shows very strong short-term fluctuations, which are presumably at least partly due to the effects of the calibration curve, and which also make this proxy seem ill-suited to reliably represent a continuous population trend. Nevertheless, its fluctuations do have an impact on the resulting overall estimate of the development of the number of settlements, albeit to a lesser extent.

6 Discussion

Our original ambition in the development of this model was to base it on a state-space representation of the demographic process itself, and then to integrate the existing proxies by means of an observation model to inform this process. In the course of developing the model, we realised that the data we had available for the case study area north of the Swiss Alps alone was not sufficient to adequately determine this process, or to adequately fix the degrees of freedom resulting from the process and the transfer model. Therefore, in implementation presented here, we have turned to a Poisson regression approach: the model represents the best possible combination of the indicators used to describe the development of the number of sites based on them.

6.1 Comparison of individual proxies

Comparing the model's overall estimate with trends indicated by individual proxies gives us new insights into the quality of these records. Sum calibration, currently the most frequently used proxy for (relative) population changes in prehistory, has its large fluctuations dampened when considered alongside other proxies. This is especially true for the first fluctuation, shortly after 4000 BCE. The expected increase in archaeological remains with the onset of Neolithisation is still clearly visible, but the curve of the overall estimate, after the initial increase, is much flatter than sum calibration alone indicates. The period between 3950 and 3700 BCE, which is contemporaneous with the first larger settlement cycle on the lakeshores of the Three Lakes region, coincides with a noticeable plateau on the calibration curve, which be producing an overestimation of the ^{14}C density. However, the effect of the calibration curve on the results of a cumulative calibration cannot yet be considered unambiguous. A second maximum, after 3000 BCE, is supported by the other proxies, and is consequently also much more clearly reflected in our overall estimate. Here, too plateau in the calibration curve — albeit a smaller, shorter one which is much less pronounced than, for example, the one shortly before between 3350 and 3100. The rise towards the Middle and Late Bronze Age is also supported by the other proxies, especially the aoristic sum, and therefore is preserved in the overall estimate. In this period, the calibration curve does not show any very clear, significant patterns. We may conclude that the model is successful in using information from other proxies to sift 'real' fluctuations in the summed radiocarbon record from artefacts of the calibration curve.

On average, the model weights the sum calibration at about 20%, significantly less than the 60% afforded to the openness indicator. After an initial increase, which is easily explained by spread of agriculture, the openness indicator tends to fluctuate less and thus has a dampening effect on the overall estimate. Nevertheless, it appears the general trends in the sum calibration are well reflected in land openness – even if such 'eyeballing' should be interpreted with caution. In contrast to this dramatic trend, changes within the Neolithic and Bronze Age are more gradual, suggestive of larger scale transformations of the landscape. The model is designed rather conservatively by the limit of maximum growth, which is estimated within the model but influences it by its very presence. Therefore, this proxy corresponds better and more homogeneously to a smooth increase in the number of settlements than do the strong fluctuations in the ^{14}C data set.

The aoristic sum remains relatively even over long spans of time. It is not until the Middle and Late Bronze Age that we see a significant rise, which is also apparent in the model's overall estimate. It remains to be seen to what extent modelling of the taphonomic loss (Surovell et al., 2009) could be integrated in this approach. We have refrained from doing so in this first model, as this would have introduced further degrees of freedom - but we are aware that with a broader database this would be an interesting possibility, and that it would itself be a variable to be estimated, e.g. in connection with proxies that are not influenced by it (openness indicators, but also data from the demography of burial collectives). This would make it possible

to estimate a value from original archaeological material independently of variables that have little to do with archaeological data, such as volcanic eruptions (Ballenger and Mabry, 2011).

The number of simultaneously existing lakeshore settlements is a very limited temporal and spatial estimator, but extremely reliable. Its limitations are reflected in the low overall confidence of the model, since its value is zero over long stretches, while other indicators suggest clearly different patterns. However, where it has information potential, such as around and shortly after 3800 BCE, 3200 BCE or especially around 2750 BCE, its fluctuations have a noticeable influence on the overall estimate. The peak around 1600 BCE also leaves a noticeable impact. This highlights another potential of our approach: where a proxy has little structure and thus little significance, or where its trends cannot be linked to other indicators, it consequently has little influence. For periods in which it can provide information, however, this will also feed into the overall model, despite a low overall confidence in the estimator.

6.2 Prehistoric population dynamics north of the Swiss Alps

In order to review the reconstruction against the background of established archaeological knowledge, it is useful to overlay conventionally-defined archaeological phase boundaries (Hafner, 2005) on the results of our model (Figure 12). It should be noted, however, that the model's estimate is not completely independent of these phases: due to the aoristic sum, which is itself strongly determined by this phase division, corresponding boundaries also influence the structure of the reconstruction. Nevertheless, it helps to check whether the estimate is in strong contradiction to the generally accepted picture or whether it is able to make a credible prediction within this context.

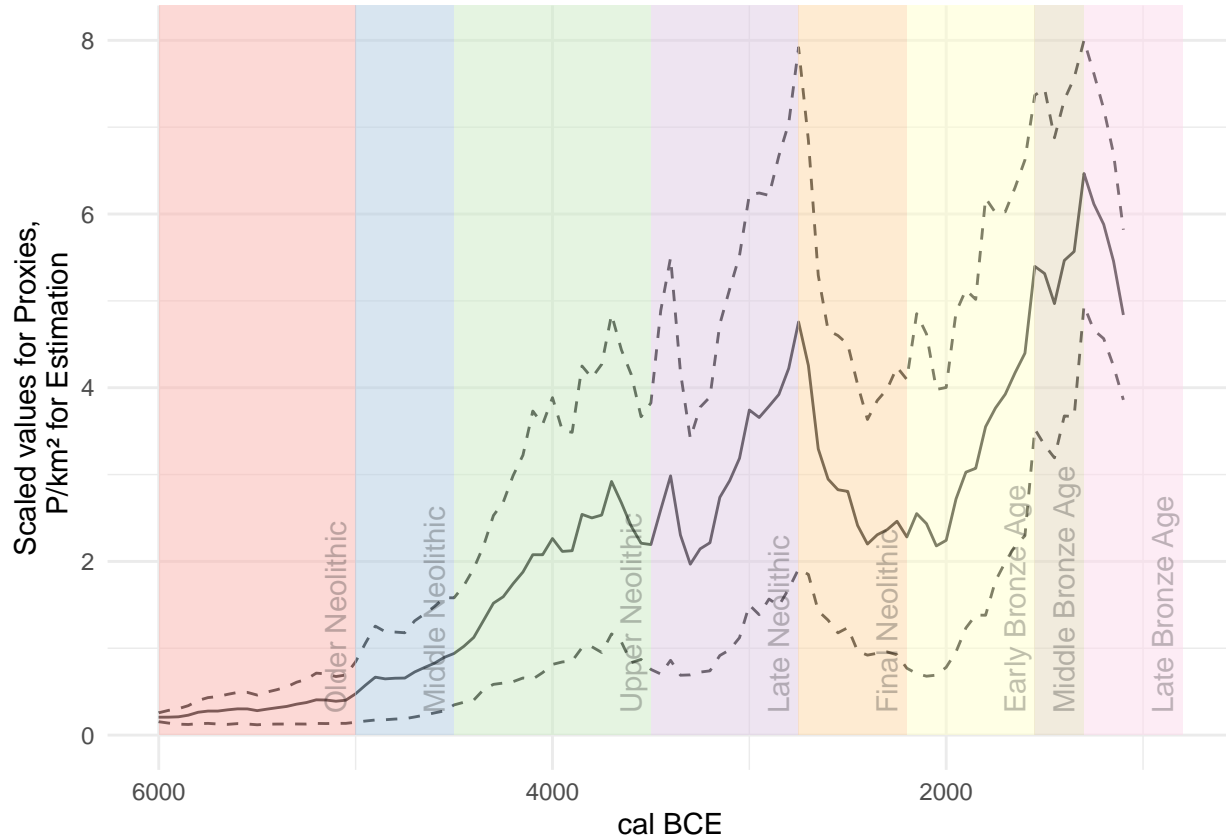


Figure 12: The estimate of the population density in relation to the chronology for the case study area north of the Swiss Alps.

The Older and Middle Neolithic phases are in fact hardly documented with known sites in Switzerland. Here we must assume a basically low level of settlement, probably mainly by hunter-gatherer groups. Isolated

Neolithic sites of the LBK and later groups are known in the periphery of Switzerland, but they play a subordinate role (Ebersbach et al., 2012). The evidence of the Neolithic especially what the Swiss Plateau is concerned is dense from the so-called Upper Neolithic onwards, connected with the typo-chronological units based on pottery that are called Egolzwil (late 5th M BCE) and Cortaillod respectively Pfyn (first half of the 4th M BCE). The first lake shore settlements north of the Alps date to this time too. In this period, we also see a clear increase in the estimated population in the model. In the transition to the Late Neolithic we know from the lakeshore settlements the so-called Horgen Gap (Hafner, 2005). This is also visible as a slight decrease in the model. In another study (Heitz et al., 2021) we could show that this is in fact probably not a decline in population. Rather communities relocated their settlements to the hinterland of the large lakes in times of lake level rises of higher magnitudes due to climatic changes. In the Late Neolithic, associated with the Horgen pottery, we then see a clear increase in the intensity of settlement, which reaches its peak and its break-off at the transition to the Corded Ware and thus to the Final Neolithic (Hafner, 2004). In the second half of the Early Bronze Age, during which – after a break from the Final Neolithic to the very early Bronze Age – lakeshores were resettled, but to a smaller extend. There is again a clear increase in population size according to the model, which continues until the Late Bronze Age. The general trends fit very well with the previous reconstructions of population development for Switzerland (see eg. Lechterbeck et al., 2014). All in all, the estimate of the model corresponds to our expectations, although we must be aware that these expectations are not ‘ground truth’. Nevertheless, we can claim that the model predictions are credible because they accord well with existing knowledge, while offering higher precision and higher resolution.

7 Conclusions

The key advance in the model we present here is the ability to estimate, in absolute terms, past population sizes and the uncertainty accompanying our present knowledge. These estimates can be used as a basis for further studies where relative measures of population development are not helpful, such as long-term land use studies, where modelling of large-scale socio-ecological systems based on archaeological data becomes possible and does have to rely on using deductive, asynchronous population models (e.g. carrying capacity or ethnographic analogues).

We have also demonstrated that, with Bayesian hierarchical modelling, it is possible to achieve a true multi-proxy analysis of prehistoric demographic processes – as opposed to a juxtaposition of different indicators. This opens up the possibility of quantitatively linking different records and assessing their credibility. In addition, and in contrast to existing approaches, we are able to specifying a confidence interval for the overall estimate. The result is a firmer basis for reconstructing population dynamics and settlement patterns in prehistory.

Nevertheless, we consider the model present here as only the first step towards a more sophisticated Bayesian approach. We have trusted the individual proxies in aggregate, without considering measurement error. Moreover, our estimates are based on a limited number of sources of evidence, almost all of which are subject to taphonomic biases in the archaeological record (except for the openness indicator). Consequently, we can only transform the model’s prediction into an absolute estimate of population density with predefined parameters: the upper limit of population growth, settlement size and the initial value of the reconstruction. Overcoming this limitation would represent a major refinement of our approach.

Incorporating additional proxies that are independent of the immediate, time-dependent conditions of the archaeological record could be one way to achieve this. These could be data on settlement sizes, parameters for economic-ecological carrying capacity, demographic data from burial groups, archaeogenetic data on population sizes, or other records as yet unidentified. This data is available to varying degrees in different regions. On the Swiss Plateau, for example, we have too little data on human remains over large spans of prehistory compared to the abundance of wetland settlements to be able to integrate them meaningful into a model.

To apply the model to different regions, the proxies we use here (e.g. the palynological openness indicator) would have to be adapted to fit local conditions and research histories. By means of large-scale modelling, however, it would be possible to supplement gaps in the data in one region with data from other regions by

means of regionalisation and a partial transfer of information (partial pooling). Such an extension would be the next logical step in the improvement of the model, to which end we hope to be able to contribute a further study in the near future.

8 Acknowledgements

Large parts of the data collection were conducted as part of the project ‘Beyond lake settlements’ in the doctoral thesis of Julian Laabs, funded by the SNF (project number 152862, PI Albert Hafner). Further data collection was done as part of the XRONOS project, also funded by the SNSF (project number 198153, PI Martin Hinz). The development of the openness index took place within the framework of the project Time and Temporality in Archaeology (project number 194326, PI Caroline Heitz) and was inspired by the cooperation within the project QuantHum (project 169371, PI Marco Conedera), both also funded by the SNSF. Jan Kolář was supported by a long-term research development project (RV67985939) and by a grant from the Czech Science Foundation (19-20970Y). We also thank the Institute of Archaeological Sciences of the University of Bern for its support and faith in the outcome of our modelling project. Finally, we thank (already) the unknown reviewers for their helpful comments, which will certainly improve this manuscript significantly.

9 References

- Attenbrow, V., Hiscock, P., 2015. Dates and demography: Are radiometric dates a robust proxy for long-term prehistoric demographic change? *Archaeology in Oceania* 50, 30–36. <https://doi.org/10.1002/arco.5052>
- Ballenger, J.A.M., Mabry, J.B., 2011. Temporal frequency distributions of alluvium in the American Southwest: Taphonomic, paleohydraulic, and demographic implications. *Journal of Archaeological Science* 38, 1314–1325. <https://doi.org/10.1016/j.jas.2011.01.007>
- Bryant, J., Zhang, J.L., 2018. Bayesian Demographic Estimation and Forecasting. Chapman; Hall/CRC. <https://doi.org/10.1201/9780429452987>
- Carleton, W.C., Groucutt, H.S., 2021. Sum things are not what they seem: Problems with point-wise interpretations and quantitative analyses of proxies based on aggregated radiocarbon dates. *The Holocene* 31, 630–643. <https://doi.org/10.1177/0959683620981700>
- Childe, V.G. (Ed.), 1936. Man Makes Himself. Watts & Co., London.
- Christian Lüthi, 2009. Mittelland (region).
- Colton, H.S., 1949. The prehistoric population of the Flagstaff area. *Plateau* 22, 21–25.
- Cook, S.F., 1946. A reconsideration of shell mounds with respect to population and nutrition. *American Antiquity* 12, 51–53.
- Cook, S.F., Heizer, R.F., 1968. Relationships among houses, settlement areas, and population in aboriginal California. *Settlement archaeology* 79–116.
- Cook, S.F., Heizer, R.F., 1965. The Quantitative approach to the relation between population and settlement size. University of California, Archaeological research facility Department of Anthropology, Berkeley, Etats-Unis d'Amérique.
- Crema, E.R., 2022. Statistical Inference of Prehistoric Demography from Frequency Distributions of Radiocarbon Dates: A Review and a Guide for the Perplexed. *Journal of Archaeological Method and Theory*. <https://doi.org/10.1007/s10816-022-09559-5>
- Crema, E.R., Bevan, A., 2021. Inference from large sets of radiocarbon dates: software and methods. *Radiocarbon* 63, 23–39. <https://doi.org/10.1017/RDC.2020.95>
- Crema, E.R., Shoda, S., 2021. A Bayesian approach for fitting and comparing demographic growth models of radiocarbon dates: A case study on the Jomon-Yayoi transition in Kyushu (Japan). *PloS One* 16, e0251695. <https://doi.org/10.1371/journal.pone.0251695>
- David-Elbiali, M., 2000. La Suisse occidentale au IIe millénaire av. J.-C. : Chronologie, culture, intégration européenne. *Cahiers d'archéologie romande*, Lausanne.
- Ebersbach, R., Kühn, M., Stopp, B., Schibler, J., 2012. Die Nutzung neuer Lebensräume in der Schweiz und angrenzenden Gebieten im 5. Jtsd. V. Chr. : Siedlungs- und wirtschaftsarchäologische Aspekte. *Jahrbuch Archäologie Schweiz* 95, 7–34. <https://doi.org/10.5169/SEALS-392483>
- Frankfort, H., 1950. Town planning in ancient Mesopotamia. *Town Planning Review* 21, 98–115.
- French, J.C., Riris, P., Fernández-López de Pablo, J., Lozano, S., Silva, F., 2021. A manifesto for palaeodemography in the twenty-first century. *Philosophical Transactions of the Royal Society B: Biological Sciences* 376, 20190707. <https://doi.org/10.1098/rstb.2019.0707>
- Hack, J.F., 1942. The changing physical environment of the Hopi Indians of Arizona, Papers of the Peabody Museum of American Archaeology and Ethnology. Harvard University, Cambridge.
- Hafner, A., 2005. Neolithikum: Raum/Zeit-Ordnung und neue Denkmodelle. *Archäologie im Kanton Bern* 6B, 431–498.
- Hafner, A., 2004. Vom Spät- zum Endneolithikum. Wandel und Kontinuität um 2700 v. Chr. In Mitteleuropa. - Vom Endneolithikum zur Frühbronzezeit: Wandel und Kontinuität zwischen 2400 und 1500 v.Chr, in: Beier, H.J., Einicke, R. (Eds.), *Varia Neolithica. 3. Beiträge Zur Ur- Und Frühgeschichte Mitteleuropas*. Beier&Beran, Weissbach, pp. 213–249.
- Hafner, A., 1995. Die Frühe Bronzezeit in der Westschweiz. Funde und Befunde aus Siedlungen, Gräbern und Horten der entwickelten Frühbronzezeit. Staatlicher Lehrmittelverlag Bern 1995, Bern.
- Hassan, F.A., 1981. Demographic archaeology, Studies in archaeology. Academic Press, New York.
- Heitz, C., Hinz, M., Laabs, J., Hafner, A., 2021. Mobility as resilience capacity in northern Alpine Neolithic settlement communities. <https://doi.org/10.17863/CAM.79042>
- Kintigh, K.W., Altschul, J.H., Beaudry, M.C., Drennan, R.D., Kinzig, A.P., Kohler, T.A., Limp, W.F., Maschner, H.D.G., Michener, W.K., Pauketat, T.R., Peregrine, P., Sabloff, J.A., Wilkinson, T.J., Wright, H.T., Zeder, M.A., 2014. Grand challenges for archaeology. *Proceedings of the National Academy of*

- Sciences 111, 879–880. <https://doi.org/10.1073/pnas.1324000111>
- Kruschke, J.K., 2015. Doing Bayesian Data Analysis. Elsevier. <https://doi.org/10.1016/B978-0-12-405888-0.09999-2>
- Laabs, J., 2019. Populations- und landnutzungsmodellierung der neolithischen und bronzezeitlichen westschweiz (PhD thesis). Bern.
- Lechterbeck, J., Edinborough, K., Kerig, T., Fyfe, R., Roberts, N., Shennan, S., 2014. Is Neolithic land use correlated with demography? An evaluation of pollen-derived land cover and radiocarbon-inferred demographic change from Central Europe. *The Holocene* 24, 1297–1307. <https://doi.org/10.1177/0959683614540952>
- Martínez-Grau, H., Morell-Rovira, B., Antolín, F., 2021. Radiocarbon Dates Associated to Neolithic Contexts (Ca. 5900 – 2000 Cal BC) from the Northwestern Mediterranean Arch to the High Rhine Area. *Journal of Open Archaeology Data* 9, 1. <https://doi.org/10.5334/joad.72>
- Morris, I., 2013. The measure of civilization: How social development decides the fate of nations. Princeton University Press, Princeton.
- Müller, J., Diachenko, A., 2019. Tracing long-term demographic changes: The issue of spatial scales. *PLOS ONE* 14, e0208739. <https://doi.org/10.1371/journal.pone.0208739>
- Naroll, R., 1962. Floor Area and Settlement Population. *American Antiquity* 27, 587–589. <https://doi.org/10.2307/277689>
- Nikulka, F., 2016. Archäologische Demographie. Methoden, Daten und Bevölkerung der europäischen Bronze- und Eisenzeiten. Sidestone Press, Leiden.
- Ramsey, C.B., 1995. Radiocarbon calibration and analysis of stratigraphy; the OxCal program. *Radiocarbon* 37, 425430.
- Rick, J.W., 1987. Dates as Data: An Examination of the Peruvian Preceramic Radiocarbon Record. *American Antiquity* 52, 55–73. <https://doi.org/10.2307/281060>
- Riede, F., 2009. Climate and demography in early prehistory: Using calibrated (14)C dates as population proxies. *Human Biology* 81, 309–337. <https://doi.org/10.3378/027.081.0311>
- Schiffer, M.B., 1987. Formation processes of the archaeological record. University of New Mexico Press, Albuquerque-NM.
- Schmidt, I., Hilpert, J., Kretschmer, I., Peters, R., Broich, M., Schiesberg, S., Vogels, O., Wendt, K.P., Zimmermann, A., Maier, A., 2021. Approaching prehistoric demography: Proxies, scales and scope of the Cologne Protocol in European contexts. *Philosophical Transactions of the Royal Society B: Biological Sciences* 376, 20190714. <https://doi.org/10.1098/rstb.2019.0714>
- Shennan, S., 2000. Population, Culture History, and the Dynamics of Culture Change. *Current Anthropology* 41, 811–835.
- Shennan, S., Downey, S.S., Timpson, A., Edinborough, K., Colledge, S., Kerig, T., Manning, K., Thomas, M.G., 2013. Regional population collapse followed initial agriculture booms in mid-Holocene Europe. *Nature Communications* 4, 2486. <https://doi.org/10.1038/ncomms3486>
- Surovell, T.A., Byrd Finley, J., Smith, G.M., Brantingham, P.J., Kelly, R., 2009. Correcting temporal frequency distributions for taphonomic bias. *Journal of Archaeological Science* 36, 1715–1724. <https://doi.org/10.1016/j.jas.2009.03.029>
- Turchin, P., Brennan, R., Currie, T., Feeney, K., Francois, P., Hoyer, D., Manning, J., Marciniak, A., Mullins, D., Palmisano, A., Peregrine, P., Turner, E.A.L., Whitehouse, H., 2015. Sesat: The Global History Databank. *Cliodynamics* 6. <https://doi.org/10.21237/C7clio6127917>
- Zimmermann, A., 2004. Landschaftsarchäologie II. Überlegungen zu prinzipien einer landschaftsarchäologie.

9.0.1 Colophon

This report was generated on 2022-05-28 10:18:46 using the following computational environment and dependencies:

```
#> - Session info -----
#>   setting  value
#>   version  R version 4.2.0 (2022-04-22)
#>   os        Manjaro Linux
#>   system   x86_64, linux-gnu
#>   ui        X11
#>   language (EN)
#>   collate   C
#>   ctype     de_DE.UTF-8
#>   tz        Europe/Zurich
#>   date      2022-05-28
#>   pandoc   2.17.1.1 @ /usr/bin/ (via rmarkdown)
#>
#> - Packages -----
#>   package * version date (UTC) lib source
#>   assertthat 0.2.1  2019-03-21 [1] CRAN (R 4.2.0)
#>   bitops      1.0-7  2021-04-24 [1] CRAN (R 4.2.0)
#>   bookdown    0.26   2022-04-15 [1] CRAN (R 4.2.0)
#>   brio        1.1.3  2021-11-30 [1] CRAN (R 4.2.0)
#>   cachem      1.0.6  2021-08-19 [1] CRAN (R 4.2.0)
#>   callr       3.7.0  2021-04-20 [1] CRAN (R 4.2.0)
#>   class       7.3-20 2022-01-16 [2] CRAN (R 4.2.0)
#>   classInt    0.4-3  2020-04-07 [1] CRAN (R 4.2.0)
#>   cli         3.3.0  2022-04-25 [1] CRAN (R 4.2.0)
#>   colorspace  2.0-3  2022-02-21 [1] CRAN (R 4.2.0)
#>   cowplot     * 1.1.1 2020-12-30 [1] CRAN (R 4.2.0)
#>   crayon      1.5.1  2022-03-26 [1] CRAN (R 4.2.0)
#>   curl        4.3.2  2021-06-23 [1] CRAN (R 4.2.0)
#>   DBI         1.1.2  2021-12-20 [1] CRAN (R 4.2.0)
#>   desc        1.4.1  2022-03-06 [1] CRAN (R 4.2.0)
#>   devtools    2.4.3  2021-11-30 [1] CRAN (R 4.2.0)
#>   digest      0.6.29 2021-12-01 [1] CRAN (R 4.2.0)
#>   dplyr       1.0.9  2022-04-28 [1] CRAN (R 4.2.0)
#>   e1071       1.7-9  2021-09-16 [1] CRAN (R 4.2.0)
#>   ellipsis    0.3.2  2021-04-29 [1] CRAN (R 4.2.0)
#>   evaluate    0.15   2022-02-18 [1] CRAN (R 4.2.0)
#>   fansi       1.0.3  2022-03-24 [1] CRAN (R 4.2.0)
#>   farver      2.1.0  2021-02-28 [1] CRAN (R 4.2.0)
#>   fastmap     1.1.0  2021-01-25 [1] CRAN (R 4.2.0)
#>   foreign     0.8-82 2022-01-16 [2] CRAN (R 4.2.0)
#>   fs          1.5.2  2021-12-08 [1] CRAN (R 4.2.0)
#>   generics    0.1.2  2022-01-31 [1] CRAN (R 4.2.0)
#>   ggmap       * 3.0.0 2019-02-05 [1] CRAN (R 4.2.0)
#>   ggplot2     * 3.3.6 2022-05-03 [1] CRAN (R 4.2.0)
#>   ggrepel     * 0.9.1 2021-01-15 [1] CRAN (R 4.2.0)
#>   ggsn        * 0.5.0 2019-02-18 [1] CRAN (R 4.2.0)
#>   glue         1.6.2  2022-02-24 [1] CRAN (R 4.2.0)
#>   gridExtra    0.3.0  2019-03-25 [1] CRAN (R 4.2.0)
#>   here        * 1.0.1 2020-12-13 [1] CRAN (R 4.2.0)
#>   highr       0.9   2021-04-16 [1] CRAN (R 4.2.0)
```

```

#> htmltools      0.5.2   2021-08-25 [1] CRAN (R 4.2.0)
#> httr          1.4.3   2022-05-04 [1] CRAN (R 4.2.0)
#> jpeg          0.1-9   2021-07-24 [1] CRAN (R 4.2.0)
#> KernSmooth    2.23-20  2021-05-03 [2] CRAN (R 4.2.0)
#> knitr          1.39    2022-04-26 [1] CRAN (R 4.2.0)
#> labeling        0.4.2   2020-10-20 [1] CRAN (R 4.2.0)
#> lattice         0.20-45  2021-09-22 [2] CRAN (R 4.2.0)
#> lifecycle       1.0.1   2021-09-24 [1] CRAN (R 4.2.0)
#> magrittr        2.0.3   2022-03-30 [1] CRAN (R 4.2.0)
#> maptools        1.1-4   2022-04-17 [1] CRAN (R 4.2.0)
#> memoise         2.0.1   2021-11-26 [1] CRAN (R 4.2.0)
#> munsell         0.5.0   2018-06-12 [1] CRAN (R 4.2.0)
#> pillar          1.7.0   2022-02-01 [1] CRAN (R 4.2.0)
#> pkgbuild        1.3.1   2021-12-20 [1] CRAN (R 4.2.0)
#> pkgconfig       2.0.3   2019-09-22 [1] CRAN (R 4.2.0)
#> pkgload          1.2.4   2021-11-30 [1] CRAN (R 4.2.0)
#> plyr            1.8.7   2022-03-24 [1] CRAN (R 4.2.0)
#> png              0.1-7   2013-12-03 [1] CRAN (R 4.2.0)
#> prettyunits     1.1.1   2020-01-24 [1] CRAN (R 4.2.0)
#> processx        3.5.3   2022-03-25 [1] CRAN (R 4.2.0)
#> proxy            0.4-26  2021-06-07 [1] CRAN (R 4.2.0)
#> ps               1.7.0   2022-04-23 [1] CRAN (R 4.2.0)
#> purrr           0.3.4   2020-04-17 [1] CRAN (R 4.2.0)
#> R6               2.5.1   2021-08-19 [1] CRAN (R 4.2.0)
#> RColorBrewer    1.1-3   2022-04-03 [1] CRAN (R 4.2.0)
#> Rcpp             1.0.8.3  2022-03-17 [1] CRAN (R 4.2.0)
#> remotes          2.4.2   2021-11-30 [1] CRAN (R 4.2.0)
#> rgdal            1.5-32  2022-05-09 [1] CRAN (R 4.2.0)
#> RgoogleMaps     1.4.5.3  2020-02-12 [1] CRAN (R 4.2.0)
#> rjson            0.2.21  2022-01-09 [1] CRAN (R 4.2.0)
#> rlang            1.0.2   2022-03-04 [1] CRAN (R 4.2.0)
#> rmarkdown         2.14    2022-04-25 [1] CRAN (R 4.2.0)
#> rnaturalearth * 0.1.0   2017-03-21 [1] CRAN (R 4.2.0)
#> rprojroot        2.0.3   2022-04-02 [1] CRAN (R 4.2.0)
#> rstudioapi       0.13    2020-11-12 [1] CRAN (R 4.2.0)
#> s2               1.0.7   2021-09-28 [1] CRAN (R 4.2.0)
#> scales           1.2.0   2022-04-13 [1] CRAN (R 4.2.0)
#> sessioninfo     1.2.2   2021-12-06 [1] CRAN (R 4.2.0)
#> sf               * 1.0-7   2022-03-07 [1] CRAN (R 4.2.0)
#> sp               * 1.4-7   2022-04-20 [1] CRAN (R 4.2.0)
#> stringi          1.7.6   2021-11-29 [1] CRAN (R 4.2.0)
#> stringr          1.4.0   2019-02-10 [1] CRAN (R 4.2.0)
#> testthat         3.1.4   2022-04-26 [1] CRAN (R 4.2.0)
#> tibble           3.1.7   2022-05-03 [1] CRAN (R 4.2.0)
#> tidyverse         1.2.0   2022-02-01 [1] CRAN (R 4.2.0)
#> tidyselect        1.1.2   2022-02-21 [1] CRAN (R 4.2.0)
#> units            0.8-0   2022-02-05 [1] CRAN (R 4.2.0)
#> usethis          2.1.5   2021-12-09 [1] CRAN (R 4.2.0)
#> utf8             1.2.2   2021-07-24 [1] CRAN (R 4.2.0)
#> vctrs            0.4.1   2022-04-13 [1] CRAN (R 4.2.0)
#> withr            2.5.0   2022-03-03 [1] CRAN (R 4.2.0)
#> wk               0.6.0   2022-01-03 [1] CRAN (R 4.2.0)
#> xfun             0.31    2022-05-10 [1] CRAN (R 4.2.0)
#> yaml             2.3.5   2022-02-21 [1] CRAN (R 4.2.0)

```

```
#>
#> [1] /home/martin/R/x86_64-pc-linux-gnu-library/4.2
#> [2] /usr/lib/R/library
#>
#> -----
```